International Journal of Science and Research (IJSR)
ISSN (Online): 2319-7064
Index Copernicus Value (2016): 79.57 | Impact Factor (2015): 6.391

Multi-Focus Image Fusion Using Discrete Cosine Harmonic Wavelet Transform

Iman M. G. Alwan

University of Baghdad, College of Education for Women, Baghdad – Iraq

Abstract: ***Multi-focus image fusion algorithms are used to combine a collection of different focuses images that represent the same scene, to produce a sharper one. In this paper, a transform domain multi-focus image fusion algorithm is proposed. It depends on using Discrete Cosine Harmonic Wavelet Transform and pixel-based rule of fusion. Region entropy is used to fuse coefficients of approximation subbands, while maximum rule with consistency verification is utilized in fusion of detail subbands of the Discrete Cosine Harmonic Wavelet Transform domain. The fused resultant image is obtained by applying inverse Discrete Cosine Harmonic Wavelet Transform to the combined coefficients.The proposed method is compared with several transform domain based fusion algorithms, and it shows better performance or similar performance under several objective criteria.***

Keywords: multi-focus image fusion, discrete cosine harmonic wavelet transforms (DCHWT), entropy region, consistency verification

1. Introduction

As imaging camera's optical lenses suffers from limited in depth-of-focus, it is impossible to hold an image with all including objects look sharp. Only the objects within the depth of field are sharp, while other objects are blurred. A common technique to obtain an image with every object in focus is the multi-focus image fusion, in which a combination of different focus setting images are fused to output a new and improved image which contains all objects are in focus. Image fusion techniques are used successfully in many fields, such as remote sensing, medical imaging, military affairs, and in surveillance. Several fusion rules are available in the open literature and these fusion strategies are categorized as: pixel-based and region-based [1].The pixel-based fusion is performed, either in the Transform Domain (TD) or Spatial Domain (SD). Each pixel (x,y) of the input images is combined by using a fusion rule and a corresponding pixel(x, y) of the fused image is formed, while in region-based, the image pixels are grouped to form contiguous regions, and the different fusion rules to each image region are applied [2]. Latterly, multi-resolution analysis has become a widely adopted technique to perform image fusion. Various transformation approaches have been developed in the literature, including the Laplacian pyramid [3], wavelet, bandelet, contourlet, and discrete cosine transform methods [4], [5], [6], [7]. In wavelet transform, the decimation of the subband components rise to interpolation, and spectral expansion of the subband signals that processed to obtain the total spectrum at the rate of original sampling produces in multiple spectral images. These specified processes of decimation and interpolation include filters of band limiting and image-rejection for eliminating aliasing, and multiple spectral images respectively. Newland [8] evolved Harmonic Wavelet Transform (HWT), he decomposed the subband in the frequency domain through gathering the coefficients of the Fourier Transform (FT), then inverting these groups to obtain the decimated signals. The subbands signals coefficients of Fourier Transform are returned to their identical places to retrieve the total spectrum at the original sampling rate. As HWT is simple and the Fast Fourier Transform (FFT) algorithm is available, this transform become very interesting. It was applied by many applications, like speech enhancement, ISAR imaging, and time/frequency analysis of digital signals [9], [10], [11]. To calculate the DFT, a rectangular window is used and due to unexpected discontinuity of it, a leakage will be produced which makes energy scattering to other HWT domain. Moreover, the processing on each single scale will influence the neighboring scales due to the processing of leaked energy too. So, the use of wavelet transformsdoesn't desire. In order to invest the HWT good characteristics, the DFT has been replaced by Discrete Cosine Transform (DCT) in applications of spectral estimation, time-frequency analysis, signal/ image compression and denoising [12], [11], [13]. An efficient and simple algorithm to compute two dimensions Discrete Cosine Harmonic Wavelet Transform has been proposed, and it is applied for application of image fusion. The experimental results show that the computation algorithm of DCHWT offers identical efficiency as that of wavelet transform based on convolution and better or similar efficiency as that of wavelets based on lifting scheme. The fusion rule depends on pixel-based fusion algorithm [14]. In this algorithm source coefficients with sharper neighborhood are chosen through calculating the weight of the them by exploiting the correlation among the coefficients at all the levels of wavelet transform domain.

In this paper, the proposed fusion algorithm based on using DCHWT for both source registered images, the combination of the approximation subband of transformed multi-focus images are done by exploiting the weighted averaging way. The entropy of region is applied to calculate the information amount from approximation subbands [15], while the combination of detail subbands depends on maximum selection rule and consistency verification step which proposed in [16].

2. Discrete Cosine Harmonic Wavelet Transform (DCHWT)

Wavelet transform is very suitable tool for analysis of some kinds of nonstationary signals, since it offers good time localization and poor frequency resolution for high frequencies, and good frequency resolution and poor time localization at low frequencies. In wavelet transformation,

Licensed Under Creative Commons Attribution CC BY

$W_x(a,b)$calculates the correlation between the input signal x(t), and $\psi(t)$which is the mother wavelet function at various scales and translations. It is given by equation (1) [17]:

$$W_x(a,b) = \frac{1}{|a|^{\frac{1}{2}}} \int_{-\infty}^{\infty} x(t)\psi^*\left(\frac{t-b}{a}\right) dt \quad (1)$$

where a is the scaling parameter, b is the translation parameter, and (*) indicate the complex conjugate. Wavelet Transform is a two variables function. If the scale is increased, the peaks of signal are likely to approximate, whereas for tails approximations, higher values of the translations are required. Myer wavelet and Shannon wavelets belong to the class of band limited wavelets; also FTs of them are propped in frequency domain in a compact manner. The scaling function ofShannon is represented in equation (2) [17]:

$$\phi(x) = sinc(x) = \frac{sin\pi x}{\pi x} \quad (2)$$

According to the theory of Parseval, equation (3) represents equation (1) in frequency domain [17]:

$$W_x(a,b) = \frac{|a|^{\frac{1}{2}}}{2\pi} \int_{-\infty}^{\infty} X(w)\Psi^*(aw)e^{jwb}\, dw \quad (3)$$

The coefficients of WT can be acquired through the application of Inverse Fourier Transform of X(w) and $\Psi^*(aw)$, as in equation (4):

$$W_x(a,b) = |a|^{\frac{1}{2}} F^{-1}[X(w)\Psi^*(aw)] \quad (4)$$

where, $X(w)$ is the FT of the signal, and $\Psi^*(w)$ is the FT of the mother wavelet successively. In Harmonic Wavelet Transform, $\Psi(w)$ is represented by equation (5).

$$\Psi(w) = \begin{cases} 1, & for\ w_c - w_0 < w < w_c + w_0 \\ 0 & elsewhere \end{cases} \quad (5)$$

As seen, the mother wavelet is a modified scaling function of Shannon. By usingw_0, w_c, the scaling and translation parameters respectively, the daughter wavelets are derived.
Hence, the HWT can be interpreted as a fiter bank with band pass filter whose bandwidths increases monotonically with their center frequencies to achieve a nearly free choise of time-frequency resolution. So, it accomplishes high time resolution and low frequency resolution in the high frequency band, and low time resolution and high frequency resolution in the low frequency bands in an adaptive manner and hence, it is proper for nonstationary signal processing. In the HWT, the decomposition of the signal is done by gathering the coefficients of the FT signal in the frequency domain by using conjugate-symmetry property. The decimated signals are obtained by applying inverse Fourier Transform for these grouped coefficients. The produced coefficients are known as Harmonic Wavelet Coefficients (HWC). After processing, a repositioning of the FTs of the subband signals,to the positions that correspond, are done to retrieve the total spectrum with rate of the original sampling process. The implementation of HWT by using Fast Fourier Transform (FFT) and Inverse Fast Fourier Transform (IFFT) can minimize the computational complexity compared to that of convolution.

Through the computation of HWCs and as an intermediate step, the coefficients of Fourier Transform are generated. These coefficients are restricted by leakage because of sudden data discontinuity which has a length of finite manner due to the existence of rectangular window in the calculation of DFT. As a result of this leakage, the energy scatter to additional scales in Harmonic Wavelet Transform and therefore processing on any one scale will influence the adjacent scales indirectly since the leaked energy gets processed too [11].

To conclude the interesting features of HWT as well as reducing the effect of leakage caused by DFT, DCT is used instead of DFT as proposed in [17]. Due to generation of periodic sequence in DCT which is even symmetric, the discontinuity is removed. The signal's symmetric extension produces double in length from that of original one, so the resolution of its frequency is best by a factor of 2. Other characteristics like energy compaction, real computational rather than complex make DCT good for applications of signal processing such as coding, denoising, and fusion.
For real symmetric signal $x_s(t)$, real symmetric $\psi_s(t)$, equation (3) will be [17]:

$$W_c(a,b) = \frac{|a|^{\frac{1}{2}}}{2,\pi} \int_{-\infty}^{\infty} X_s(\omega)\Psi_s(a\omega)\cos(\omega b)\, d\omega \quad (6)$$

$X_s(\omega)$, $\Psi_s(\omega)$ are the cosine transforms of $x_s(t)$ and wavelet function$\psi_s(t)$ respectively. Equation (4) can be rewritten as:

$$W_c(a,b) = |a|^{1/2} C^{-1}[X_s(\omega)\Psi_s(a\omega)] \quad (7)$$

As $\Psi(\omega)$ which is the function of harmonic wavelet in HWT domain, $\Psi_s(\omega)$ which represents the function of cosine harmonic wavelet is simple also its value equal to constant at small frequency bands while its value is zero for all other frequencies. Equation (8) represents it [17].

$$\Psi_s(\omega) = \begin{cases} 1, & \omega_c - \omega_0 < \omega < \omega_c + \omega_0 \\ -\omega_c - \omega_0 < \omega < -\omega_c + \omega_0 & \\ 0 & elsewhere \end{cases}$$

In DCHWT, the decomposition of the input signal is done by gathering the coefficients of DCT like coefficients of DFT except the operation of conjugate in putting the coefficients in symmetric manner (because DCT is real). By applying inverse discrete cosine transform for these groups, the Discrete Cosine Harmonic Wavelet coefficients are produced. DCHWT has features such as pliancy of built-in decimation process as well interpolation process, DCT fast algorithm include real operations only so it is easier than convolution [17]. The 2D DCHWT steps for one level of decomposition are stated as follows [14]:

Input: signal to be decomposed X (N, N)
Output: DCHWT of input signal.
1- Calculate 2D DCT of the input signal X (N, N)

Licensed Under Creative Commons Attribution CC BY

2- Collect the coefficients of the two dimension DCT as four groups which are Gr1, Gr2, Gr3, and Gr4. Each of size ($\frac{N}{2} \times \frac{N}{2}$). This is shown in Figure 1.
3- Apply the 2D IDCT for each group. Gr1 gives the approximation suband A1, Gr2 gives the vertical subband V1, Gr3 gives the horizontal subband H1, and Gr4 gives the diagonal subbands D1.

End

To reconstruct the 2D signal from the DCHWT domain again, after processing the 2D DCHWT coefficients of each subband, the previous steps are retraced back to retrieve the total spectrum of discrete cosine transform, the result is applied to reset the 2D signal by applying the 2D IDCT.

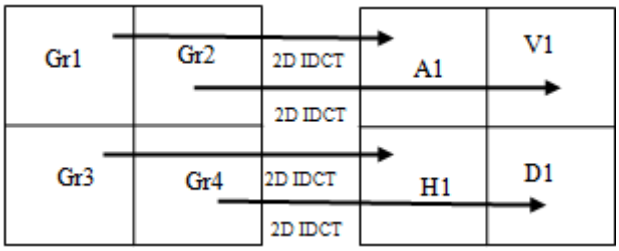

Figure 1: 2D DCHWT

3. Image Fusion Process

In frequency domain, Image fusion process is originally achieved through applying appropriate transform and through specific criteria for choosing of detail subbands coefficients to be fused and approximation subband coefficients to be fused respectively.

3.1.Detail Subbands Combination

Since high frequency presents contour and shape feature of image, conventional way ordinarily chooses maximum absolute values of high frequency coefficients. As the image's valuable features are usually greater than one coefficient, the rule of maximum selection may not be convenient method. Latterly, measurements such as, Energy of Laplace (EOL), Energy of Gradient (EOG), Sum Modified Laplacian (SML), and Spatial Frequency (SF) have been applied in the fusion of detail subbands [18]. In this paper, a method proposed in [16] is adopted. In this method, a maximum absolute value within a window of 3x3 or 5x5 is used as an activity measure related with the center pixel in all subbands of wavelet domain. In this technique, the existence of a dominant feature in the local area is indicated by the high activity value. A binary decision map is built to register the selection results; it is of the same size as the transformed images to be fused. The binary map is utilized in consistency verification. In the wavelet domain, if the value of center pixel arrives from image X while the majority of pixel values that surround the central pixel come from image Y, the value of center pixel is turned to that of image Y. The majority filter is used in consistency verification window-based system. It is given by equation (9) [18]:

$$Dm_b = \begin{cases} 1, & if\ Dm * W_i > \frac{i^2}{2} \\ 0, & otherwise \end{cases} \quad (9)$$

where Dm is the input decision map, Dm_b is the filtered decision map, W_i is a sliding matrix of *ixi* dimension with all values equal to 1. This method is exploited in fusion of details subbands outputted from DCHWT stage.

3.2. Approximation Subband Combination

The approximation subbands of the transformed input images are joined. Generally, approaches of averaging the input approximation subbands is used but this causes contrast reduction in opposite contrasts of different source images [1]. In this paper, the proposed algorithm invests a weighted average process to generate the fused approximation coefficients of the highest decomposition level. To calculate the amount of information from approximation subbands that contribute to the fused result, the region entropy [15] is utilized. The region entropy is measured for every coefficient in approximation band by using its corresponding coefficient (child) in every detail subbands at all orientations for all levels. Equation (11) represents the approximation fused coefficient which denoted as $C_f^l(I)$ [19]:

$$C_f^l(I) = \frac{E_x(I)}{E_x(I)+E_y(I)} C_x^l(I) + \frac{E_y(I)}{E_x(I)+E_y(I)} C_y^l(I) \quad (10)$$

$$E_x(I) = \sum_L \sum_\theta \sum_{i \in \Omega_k} C_x^{L,\theta}(i) \log(C_x^{L,\theta}(i))^2 \quad (11)$$

$$E_y(I) = \sum_L \sum_\theta \sum_{i \in \Omega_k} C_y^{L,\theta}(i) \log(C_y^{L,\theta}(i))^2 \quad (12)$$

where, $C_x^l(I)$, $C_y^l(I)$ are the approximation coefficient of two source images. $E_x(I)$, $E_y(I)$ are the region activity measures for the two source images *X*, *Y* respectively at the position *I* using the corresponding coefficients of detail subbands over all levels (L) and all orientations (θ).

4. The Proposed Fusion Algorithm

The proposed algorithm collects images from multiple sources to reconstruct a single image from these which are captured at various focus levels. Firstly, DCHWT is applied for each input image. Then the approximation and the detail DCHWT coefficients are combined using different pixel-level fusion rules. For approximation subbands, the method of section 3.2 is used. This fusion process depends on investing a weighted averaging method to output the combined approximation coefficients. The combination of the detail subbands is as method of section 3.1. It depends on rule of maximum chosen with consistency verification. Finally, the fused image is got by implementing the inverse of DCHWT on the fused transform domain coefficients.

The steps of the proposed algorithm are provided as follows:
Input: Multi-focus images X, Y.
Output: Fused image F.

1) Apply one dimension DCHWT on registered source images X and Y.
2) For each detail subband (V_1, H_1, D_1) of images X, Y respectively
   - Specify the maximum absolute value within 3x3 window as a measure of activity associated

Licensed Under Creative Commons Attribution CC BY

- Create a binary decision map of the same size as every detail subband (V_1, H_1, D_1) of X, Y images to record the selection results.
- Apply the majority filter as in equation (9) to the binary decision map, then negate the map.
- Add each detail subband of image X with the corresponding one of image Y after multiplying the first one with the filtered decision map and the second one with the negated filtered decision map. The fused detail subbands (V_f, H_f, D_f) is obtained.

3) For approximation subband (A_1) of both images X, Y respectively, combine each coefficient using equation (10) to get A_f .
4) Apply inverse DCHWT to get the fused image F.
5) End.

4. Fusion Performance Measure

In most applications, the reference images are not available; this makes the evaluation of fusion performance a difficult task. Different parameters are proposed and utilized to evaluate fusion performance. They are listed as follows [14, 20]:

1- Average Pixel Intensity (API) or mean $(\bar{M})$: contrast measurement, it is given by

$$API = \bar{F} = \frac{\sum_{a=1}^{m}\sum_{b=1}^{n} f(a,b)}{mxn} \quad (13)$$

where, $f(a,b)$ is intensity of pixel at *(a,b)*,mxn is the image size.

2- Standard Deviation(SD): square root of the variance, it points to the diffusion of data.

$$SD = \sqrt{\frac{\sum_{a=1}^{m}\sum_{b=1}^{n}(f(a,b)-\bar{F})^2}{mxn}} \quad (14)$$

3- Average Gradient (AG): reflects the lucidity degree and sharpness

$$AG = \frac{\sum_a \sum_b {((f(a,b)-f(a+1,b))^2+(f(a,b)-f(a,j+1))^2)}^2}{mxn} \quad (15)$$

4- Entropy (E): estimates the amount of information present in the image

$$E = -\sum_{i=0}^{255} p_i log_2 (p_i) \quad (16)$$

where p_i represent the probability of intensity value i in grey scale image.

5- Mutual Information (MI): determine the total mutual information between source images and fused one.

$$= MI_{XF} + MI_{YF} \quad (17)$$

where, MI_{XF} , MI_{YF} represent the mutual information between source image *X*, source image Y and the fused image *F* respectively.

$$MI_{XF} = \sum_x \sum_f p_{X,F}(x,f) log_2 \frac{p_{X,F}(x,f)}{p_X(x)p_F(f)} \quad (18)$$

$$MI_{YF} = \sum_y \sum_f p_{y,F}(y,f) log_2 \frac{p_{Y,F}(y,f)}{p_Y(y)p_F(f)} \quad (19)$$

6- Fusion Symmetry (FS): denote the symmetric magnitude between fused image and source images.

$$FS = 2 - \left|\frac{MI_{XF}}{MI} - 0.5\right| (20)$$

7- Correlation Coefficient (CC): calculate the relation of fused image to source ones.
$CC = (cr_{XF} + cr_{YF})/2 (21)$
where,

$$cr_{XF} = \frac{\sum_i \sum_j \left(x_{(i,j)}-\bar{X}\right)(f_{(i,j)}-\bar{F})}{\sqrt{(\sum_i \sum_j (x_{(i,j)}-\bar{X})^2)\sum_i \sum_j (f_{(i,j)}-\bar{F})^2)}} (22)$$

$$cr_{YF} = \frac{\sum_i \sum_j \left(y_{(i,j)}-\bar{Y}\right)(f_{(i,j)}-\bar{F})}{\sqrt{(\sum_i \sum_j (y_{(i,j)}-\bar{Y})^2)\sum_i \sum_j (f_{(i,j)}-\bar{F})^2)}} (23)$$

8- $Q^{XY/F}$ parameter: calculate the whole information that transferred from source images to fused image.

9- $L^{XY/F}$, parameter: calculate the loss in edge information.

10- $N^{XY/F}$ parameter: calculate the noise or artifacts appended to the fused image by the fusion process.

The parameters (8-10) were proposed by Petrovic and Xydeas [20]. They are based on gradient information. If reference image is available, one can use PSNR criteria to measure the performance of the fusion process. It is stated as [18]:

$$PSNR = 10log_{10}(\frac{255^2}{MSE}) (24)$$

$$MSE = (\frac{1}{N})^2 \sum\sum(p_{ij} - p'_{ij})^2 (25)$$

where p_{ij} 's stand for the values of the original pixel, p'_{ij} 's stand for the values of the modified pixel, and N is the image dimension.

5. Experimental Results and Analysis

To evaluate the proposed algorithm, it is compared with one level 'db1' wavelet based fusion system and with fusion system based on DCHWT proposed by Kumar [14]. Also, the results are compared with the algorithm proposed by Haghighat, et.al. in [7] which based on DCT + variance and consistency verification method and with the algorithm proposed by Tian and Chen in [21] in which the measurement of the blurring in the image depends on a new statistical sharpnessmeasure based on the diffusion of the wavelet coefficients distribution. Experiments were implemented on different standard (256x256)gray-scale test pairs of multi-focus images which obtained from (imgfsr.com) where the reference images are not obtainable, so the metrics of section 5 are used to evaluate the performance. Since reference images isn't obtainable; the measurement of how much the fused image is close to perfect is difficult. Therefore, a second experiment is executed on images of various focus levels generated artificially. Four images are used(Girl, House, Boat, and Clock), which represent ground truth. The generation of the blurred images is implemented by applying average filter of

Licensed Under Creative Commons Attribution CC BY

7x7 window for left side and right side of the four test images. PSNR metric is used to calculate the performance of the proposed algorithm and other fusion ones.

Experiments are executed by using MATLAB Version 7.0.4.365, with processor of Intel core i7, 2.7 GHz and 4G RAM. Figure 2 shows the test multi-focus images and the outputted fused images of the first experiment where no reference images are available. Table 1 (a,b) , presents the evaluation results of the proposed algorithm and wavelet based algorithm and algorithms of Kumar, Haghighat et. al, and Tian and Chen respectively. The implementation of these algorithms is done by the programs supplied by their authors. Figure 3 represents the blurred images artificially. Table 2 shows the PSNR comparison results of the proposed algorithm and the four other algorithms.

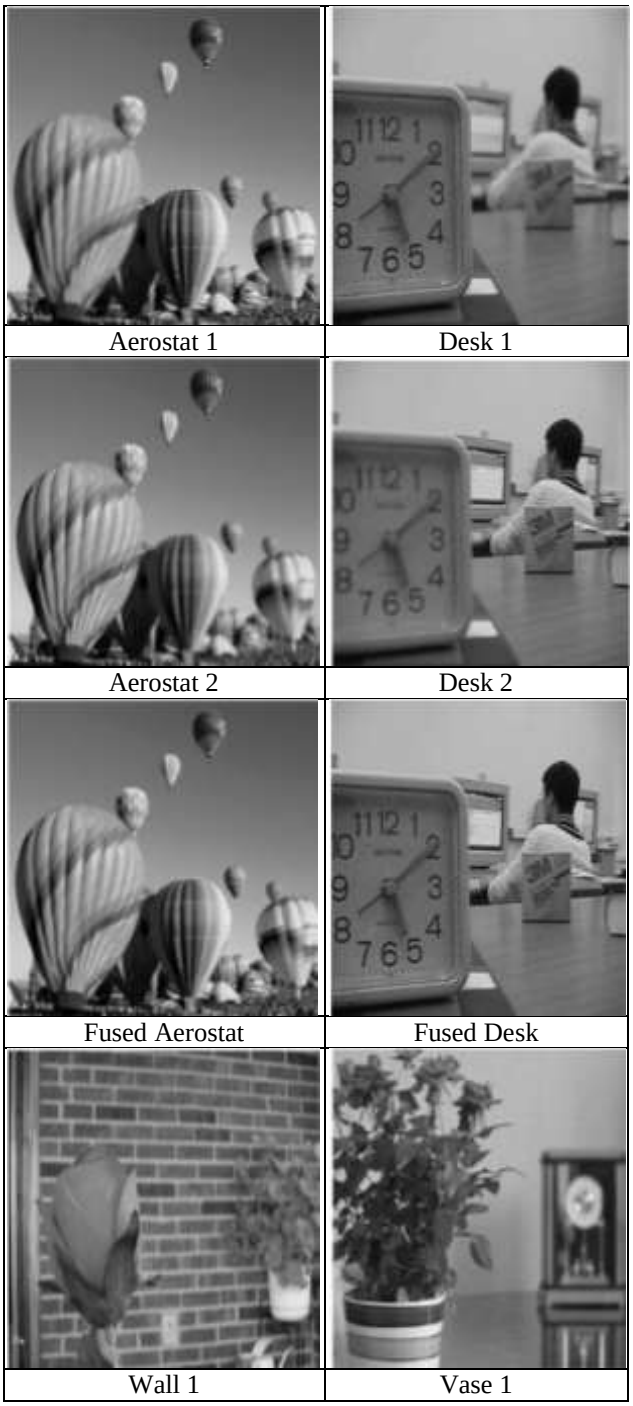

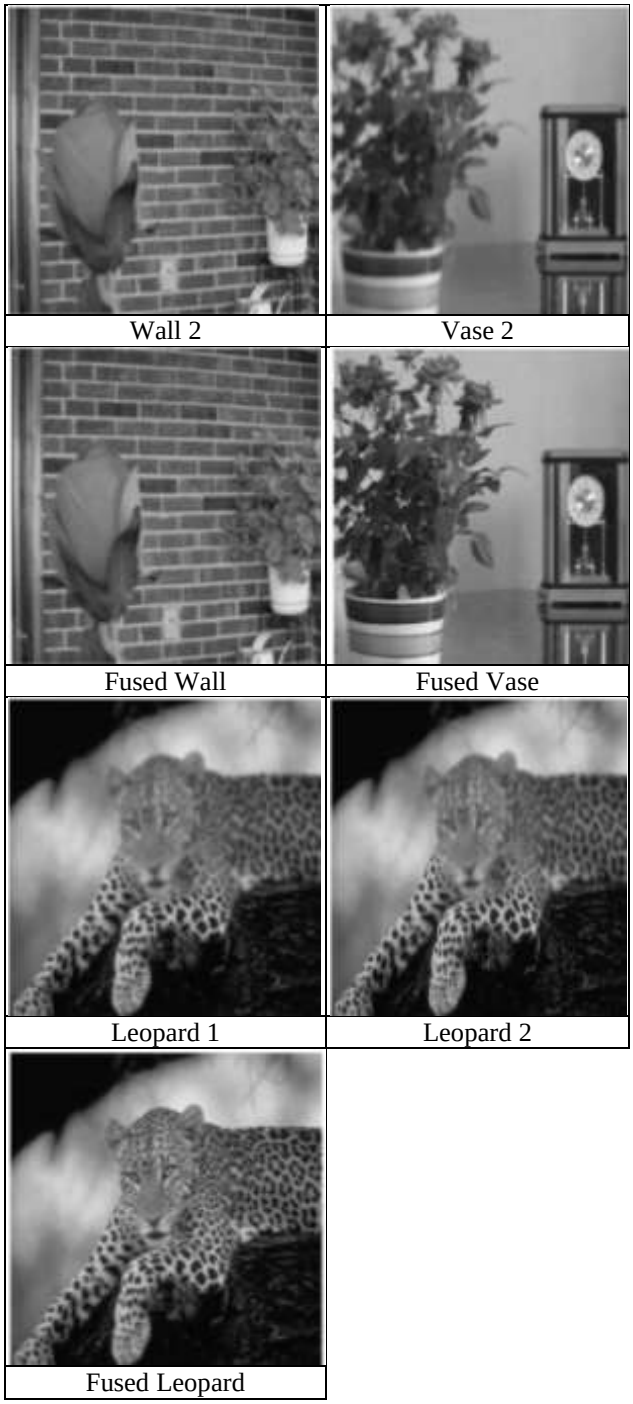

Figure 2: The multi-focus test images, and the outputted fused image

Licensed Under Creative Commons Attribution CC BY

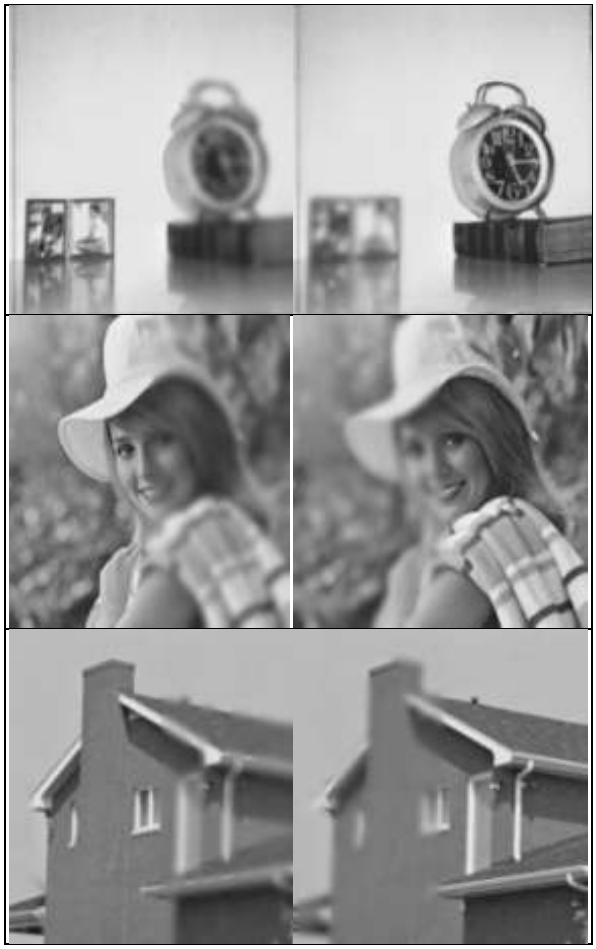

Figure 3: Multi-focus test images generated artificially

Table 1 (a): Performance Evaluation of The Proposed Fusion System

Desk	API	SD	$\bar{G}$	E	MI
Proposed	122.6079	**46.6758**	**8.4996**	**7.0364**	8.4419
WT	122.632	46.6400	8.4437	7.0127	8.5518
[14]	**122.7819**	45.7978	7.7717	7.0198	7.5901
[7]	122.6461	46.3978	8.3248	6.9810	**8.9109**
[21]	122.5711	46.6366	8.3805	7.0327	8.5379
Wall					
Proposed	103.1896	**35.1961**	**15.8724**	**7.0968**	7.8801
WT	103.7562	35.0031	15.5276	7.0933	7.4665
[14]	**105.1590**	34.5576	14.4118	7.0795	6.2842
[7]	104.1980	35.0353	15.2131	7.0958	**8.0892**
[21]	103.4440	35.0670	15.4757	7.0939	7.6980
Vase					
Proposed	**114.3153**	**51.1376**	**11.8808**	**7.5117**	8.3375
WT	114.2240	50.9265	11.7357	7.4148	1.8967
[14]	113.8755	50.1329	10.896	7.3705	6.8160
[7]	114.0619	50.6749	11.588	7.4136	**8.7030**
[21]	114.0221	51.027	11.6545	7.4139	8.3212
Aerostat					
Proposed	**113.7454**	**45.9847**	**11.0073**	**7.4539**	11.225
WT	113.7431	45.9503	10.9818	7.4530	11.5217
[14]	113.5692	45.3441	10.3761	7.4394	10.2329
[7]	113.7111	45.9374	10.9853	7.4524	**11.6010**
[21]	113.7406	45.952	10.956	7.4520	11.4429
Leopard					
Proposed	**92.2860**	**64.5686**	**14.5147**	**7.3583**	10.2478
WT	92.2850	64.558	14.4844	7.3504	11.0169
[14]	92.1616	63.8856	13.4801	7.3618	8.9040
[7]	92.2670	64.5337	14.4717	7.3498	**11.1161**
[21]	92.2814	64.5601	14.472	7.3510	10.9095

Table 1 (b): Performance Evaluation of The Proposed Fusion System

Desk	FS	CORR	$Q^{XY/F}$	$L^{XY/F}$	$N^{XY/F}$
Proposed	1.985	0.9856	0.8969	0.0940	0.0497
WT	1.9897	0.9895	0.8965	0.0992	0.0210
[14]	**1.9993**	**0.9927**	**0.9170**	**0.0816**	0.0071
[7]	1.9975	0.9895	0.8919	0.1063	**0.0050**
[21]	1.9948	0.9896	0.8967	0.0990	0.0265
Wall					
Proposed	1.7942	0.9807	0.9486	0.0495	0.0080
WT	1.8334	0.9742	0.9479	0.0493	0.0107
[14]	**1.9295**	**0.9828**	**0.9701**	**0.0295**	0.0041
[7]	1.8632	0.9728	0.9519	0.0475	**0.0017**
[21]	1.8137	0.9748	0.9505	0.0469	0.0112
Vase					
Proposed	1.9043	0.9800	0.8823	0.1144	0.0190
WT	1.8967	0.9836	0.8787	0.1188	0.0135
[14]	**1.9505**	**0.9866**	**0.9025**	**0.0958**	0.0080
[7]	1.9116	0.9831	0.8827	0.1164	**0.0030**
[21]	1.8953	0.9832	0.8829	0.1139	0.0167
Aerostat					
Proposed	1.9978	0.9955	0.9796	0.0192	0.0046
WT	1.9900	0.9966	0.9796	0.0202	$5.9*10^{-4}$
[14]	1.9971	**0.9973**	**0.9861**	**0.0137**	$9.64*10^{-4}$
[7]	1.9990	0.9967	0.9798	0.0202	$\mathbf{8.17*10^{-6}}$
[21]	**1.9996**	0.9966	0.9797	0.0198	0.0021
Leopard					
Proposed	1.9588	**0.9943**	0.9519	0.0420	0.0316
WT	1.9593	0.9898	0.9518	0.0481	$4.96*10^{-4}$
[14]	**1.9816**	0.9915	**0.9669**	**0.0326**	0.0025
[7]	1.9626	0.9898	0.9517	0.0483	$\mathbf{6.22*10^{-5}}$
[21]	1.9606	0.9898	0.9519	0.0468	0.0063

Table 2: PSNR (dB) for proposed fusion algorithm and other fusion methods

Test image	Boat	Clock	*Girl*	House
Proposed	**42.70**	**35.09**	**46.70**	**41.41**
WT	42.58	34.95	46.65	41.36
[14]	39.64	34.69	42.95	39.32
[7]	40.99	34.88	43.11	39.60
[21]	42.64	35.07	46.61	41.37

In theory, greater values of parameters (1-8) in section (5) mean best quality of the obtained fused image, while values of parameters (9-10) should be minimum. In Table 1, greater values are bolded except for L_{XYF}, N_{XYF} where lower values are bolded. From the results of Table 1, it's noticed that the proposed algorithm offers better performance in term of (SD), (AG) and (E) for all test images, while it performs better performance for three test images in terms of (API). The algorithm proposed by Haghighat et. al. offers better performance in terms of Mutual Information (MI) and $N^{XY/F}$ parameter, while the algorithm proposed by Kumar offers better performance in terms of Correlation (CC), $Q^{XY/F}$, and $L^{XY/F}$ parameters respectively. Hence,the proposed algorithm offers similar\higher performance in few tenths from the other proposed algorithms. In Table 2, where reference image is available, results of PSNR show that the proposed algorithm offers better results among other fusion algorithms.

6. Conclusions

In this paper, an algorithm of multi-focus image fusion in transform domain is proposed. This algorithm bases on

Licensed Under Creative Commons Attribution CC BY

employing DCHWT in fusion process by decomposing the input multi-focus images into one-level DCHWT, and then using maximum-rule with consistencyverification for detail subbands and weighted average process depending on region entropy for approximation subbands. The simulation results exhibit better or similar execution as compared with other algorithms in terms of quantitative parameters and visual quality.

References

[1] I. Alwan, "Multi-Focus Image Fusion Based on Pixel Significance Using Contourlet Transform", *Al-Khwarizmi Engineering Journal*,vol. 11, no.3,pp. 85-95, 2015.
[2] N. Mitianoudis, and T. Stathaki , "Pixel-based and region-based image fusion schemes using ICA bases", *Information Fusion*, vol. 8, no.2, pp.131–142, 2007.
[3] Wang,W. and Chang, F., "A multi-Focus Image Fusion Method Based on Laplacian Pyramid", *journal of computer*, vol. 6,no. 12, pp. 2559-2566, 2011.
[4] L. Yu , W. Zengfu, "Multi-focus Image Fusion Based on Wavelet Transform and Adaptive Block", *Journalof Image and Graphics*, vol.18.no.,11,pp. 1435-1444, 2013.
[5] Qu,X., Yan,J., Xie,G., Zhu, Z., and Chen, B., "A Novel Image Fusion Algorithm Based on Bandelet Transform", Chinese Optic Letters, vol.5,no. 10,pp. 569-572, 2007
[6] M. Qiguang, ,"A Novel Image Fusion Method Using Contourlet Transform", Communication, Circuits, and Systems Proceedings, International Conference, pp. 25-28, June, 2006.
[7] M. Haghighat, A. Aghagolzadeh, and H. Seyedarabi, "Multi-focus fusion for visual sensor networks in DCT domain", Computers and Electrical Engineering vol.37, pp. 789-797, 2011.
[8] D. E. Newland, " Harmonic Wavelet Analysis", In: Proc. of the Royal Society of London A: Mathematical, Physical and Eng. Sciences, 443(1917),pp. 203-225, 1993.
[9] T. Gurlzow , T. Ludwig, U. Heute , " Spectral-subtraction Speech Enhancement in Multirate Systems with and without Non-uniform and Adaptive Bandwidths", *Signal Process*, Vol.83,no.8 , pp. 1613-1631, 2003.
[10] B. K. Shreyamsha Kumar, Prabhakar, B., Suryanarayana, K., Thilagavathi, V., "Harmonic Wavelet Based ISAR Imaging for Target Identification*", Proc. of Int. Radar Symposium India(IRSI)*, Bangalore, India, pp. 343-348, Dec., 2005.
[11] S. V. Narasimhan, B. K. Shreyamsha Kumar, " Harmonic Wavelet Transform Signal Decomposition and Modified Group Delay for Improved Wigner-Ville Distribution", Int. Conf. on Signal Process. and Communications (SPCOM), Bangalor, India, pp. 354-358, Dec., 2004.
[12] S.V. Narasimhan, M. Harish, "Discrete Cosine Harmonic Wavelet Transform and its Application to Subband Spectral Estimation using Modified Group Delay*", Proc. Of Conf. in honor of Dr. B. R. Pai,* National Aerospace Laboratories, Bangalore, India, Nov., 2004.
[13] B. K. Shreyamsha Kumar ," Image Denoising using Discrete Cosine Harmonic Wavelets" *Technical Report, Sensor Signal Process. Group*, Central Research Laboratory, Bangalore, India, Jul., 2010.
[14] B. K. Shreyamsha Kumar., "Multifocus & Multispectral Image Fusion Based on Pixel Significance Using Discrete Cosine Harmonic Wavelet Transform", *Signal, Image, and VideoProcessing*, vol. 7, no. 6, pp 1125-1143, 2013.
[15] T.Wan, N. Canagarajah, and A. Achim" Segmentation-driven image fusion based on Alpha-stable modeling of wavelet coefficients", *IEEETransactions on Multimedia*, vol. 11 pp. 624–633, 2009.
[16] H.Li, , B.S. Manjunath, S.K. Mitra, " Multisensor image fusion using the wavelet transform", *Graphical Models and Image Processing*, vol. 57, no. 3, pp. 235-245, 1995.
[17] S. V. Narasimhan, M. Harish,A. R. Haripriya A. R., and N. Basumallick, "Discrete Cosine Harmonic Wavelet Transform and its Application to Signal Compression and Subband Spectral Estimation using Modified Group Delay", *J. SIViP*, vol. 3, no.1, pp. 85-99, 2009
[18] Lu.H., L. Zhang, .,and S. Serikawa, "Maximum local energy: An effective approach for multisensor image fusion in beyond wavelet transform domain", *Computers and Mathematics with Applications*, vol.64,no.5,pp.996-1003, 2007.
[19] Zhan,K., Teng,J., Li,Q., and Shi,J., " A Novel Explicit Multi-focus Image Fusion Method",*Journal of Information Hiding and Multimedia SignalProcessing*, vol.6, no. 3,pp.600-612, 2015.
[20] V. Petrovic, C. Xydeas, "Objective Image Fusion Performance Characterization", Proceedings of ICCV'05, vol. 2, pp. 1866-1871, 2005.
[21] J.Tian, L. Chen, "Adaptive multi-focus image fusion using a wavelet-based statistical sharpness measure", *Signal Processing Journal*, vol.92, no. 9, pp.2137-2146, 2012.

Licensed Under Creative Commons Attribution CC BY